1. Nuruliswa ABDULLAH[1], 2. Mohamad Z. A. ABD. AZIZ[1], 3. Abd SHUKUR JAAFAR[1]

Universiti Teknikal Malaysia Melaka (1)
ORCID. 1. 0000-0001-7549-0671, 2. 0000-0002-9926-158X, 3. 0000-0002-4821-2411

doi:10.15199/48.2021.10.02

Design of a high directive sensor for microwave imaging application

Abstract*. This paper presents a compact uniplanar Vivaldi antenna sensor for microwave imaging. It is ideal for microwave imaging systems with its large bandwidth and end-fire radiation performance. The Vivaldi patches integrate a coplanar waveguide (CPW) feed line, ensuring the entire structure is compact and simple. Reflection coefficient, radiation pattern, gain, efficiency, and directivity were the antenna parameters analyzed to determine the Vivaldi antenna's performance. The bandwidth of the antenna sensor is wider, approximately 5 GHz (3-8 GHz). The gain of the antenna is 6.72 dBi, and the directivity is 9.59 dBi.*

Streszczenie. *W artykule przedstawiono kompaktowy jednopłaszczyznowy czujnik antenowy Vivaldiego do obrazowania mikrofalowego. Jest idealny do systemów obrazowania mikrofalowego dzięki dużej szerokości pasma i wydajności promieniowania końcowego. Łaty Vivaldi integrują współpłaszczyznową linię zasilającą falowodu (CPW), zapewniając, że cała konstrukcja jest zwarta i prosta. Współczynnik odbicia, charakterystyka promieniowania, wzmocnienie, wydajność i kierunkowość były parametrami anteny analizowanymi w celu określenia wydajności anteny Vivaldi. Szerokość pasma czujnika anteny jest szersza, około 5 GHz (3-8 GHz). Zysk anteny wynosi 6,72 dBi, a kierunkowość 9,59 dBi. (**Projekt czujnika o wysokiej kierunkowości do aplikacji obrazowania mikrofalowego*)

Keywords: microwave imaging system, CPW feed, vivaldi antenna, directivity,
Słowa kluczowe: obrazowanie mikrofalowe, pasza CPW, antena Vivaldiego, kierunkowość,

Introduction

Microwave imaging introduces a complementary fast and non-ionizing method to the existing techniques such as X-ray, mammography, ultrasound, Computed Tomography (CT) scan, and Magnetic Resonance Imaging (MRI) that are either expensive and bulky or based on ionizing radiations. As a consequence of mammography using ionizing radiation, painful breast compression is required during the breast examination. Furthermore, mammography ionization has many side effects that paradoxically risk malignancy in healthy cells. Besides, deep cancer cells are difficult to identify. Magnetic Resonance Imaging (MRI) produces high-resolution images. The cost of an MRI machine is also exorbitant [1]. Physicians are currently using the computed tomography (CT) and MRI as stroke detection devices. The CT will confirm the stroke diagnosis and inform whether a brain hemorrhage causes the stroke. MRI is used to detect and locate the stroke's site and source. An ischemic stroke can be easily detected. However, these two tools are expensive and not always available [2]. Both are massive and cannot be transported by paramedic teams as the first responder. Microwave imaging can be replicated better than conventional systems since it is free of ionizing radiation compared to existing imaging systems. Recently, microwave imaging technologies have found applications in significantly different sub-surface sensing medical imaging, non-destructive testing and evaluation (NDT&E), and security screening system. Disadvantages and limitations of existing detection techniques motivated researchers to investigate and develop new microwave-based imaging techniques. Three configurations were explored for microwave imaging based on the radar-based technique. The configurations of the three radar-based techniques are monostatic, bistatic, and multistatic.

A monostatic configuration is a single antenna in which a transmitter (Tx) and a receiver (Rx) are collocated [3]. The receiver can collect the information from the transmission or reflection signal. This configuration only depends on the reflected signal and covers a small section area if the antenna's position is static. However, the antenna can be non-static where it displaces the circularly cover area and sends more data within the operating frequency band to the receiver [4]. This approach aims to use backscattering signals to produce images that detect the presence of an embedded object recorded at 144 different angular positions [5]. The monostatic configuration can also cover all areas if the object is rotated when the antenna is fixed position [6]. Within this movement, the data was automatically acquired at 44 locations [7]. The other proposed antenna moves along the object to scan all areas [8].

Next, the bistatic configuration has two antennas, where the positions of Tx and Rx are separated by a distance comparable to the expected target distance [9]. This configuration is static and only covers one cross-section area. The receiver can collect the information from the transmission or reflection signal. The antennas are placed face to face at a distance and in a static position, and the breast phantom rotates at 120 equivalence point with a 3-degree of separation [10]. Hence, [11] presented the non-static configuration for both antennas that can move independently on their track by rotating at 24 x 19 data collection. However, [12] showed only Rx moves while Tx is static where the target data are collected for 26 evenly spaced receiving antenna points. Some of these configurations used either reflection [13] or transmission [14], and others used the combination of transmission and reflection [11] for data collection. Both configurations for monostatic and bistatic can also cover all areas if the antenna or the object is rotating, but it is time-consuming. This setback can be eliminated if the multistatic configuration is utilized.

Multistatic configuration means having more than two antennas [15], and it has three approaches. Some of these multistatic configurations use a static or non-static antenna. The first approach is monostatic where it uses reflection [16]. It is used in one antenna for Tx and Rx and applied to other antennas. The second approach is bistatic, in which the transmission between antenna 1 and 2 occurs while the electric field is transmitted through the object [17]. Antenna 1 or 2 can serve as a transmitter, while the other antenna should be used as a receiver.

Subsequently, the third approach is multistatic; it can be a single Tx and multiple RX, multiple Tx and single Tx, or multiple Tx and multiple RX configurations. For this configuration, the static antenna position is most used. The transmission used in this multistatic configuration is either transmission or reflection, but others used the combination of transmission and reflection. [18] presented 16 antennas

in static positions with array configurations (regular cross, regular ring, asymmetrical regular, and asymmetrical irregular). The proposed array has 16 static antennas [19] where one is the TX and other antennas act as the RX and collect 240 multistatic signals. [20] put forward 20 elements array antenna in a static position and proposed using a reflection coefficient in the array configuration.

Antenna sensors play a vital role in microwave imaging systems, where the antenna serves as a transmitting and receiving sensor. A microwave imaging system involves transmitting microwave signals through the objects and receiving the scattered signals from different locations. The technique can detect and locate abnormalities inside the object from the reflected and scattered signals of the object. Eventually, through the advancement of technology, the criteria for success are modifications for optimal imaging results. Antenna sensors with high gain, directive design, and higher efficiency are required for microwave imaging applications. Various types of antenna sensors have been proposed for microwave imaging applications, namely horn [21], slotted patch [22], bowtie antenna [3], coplanar waveguide CPW , and Vivaldi. Several design use monopole for enhance the performance of the antenna to get the UWB frequency range [24]–[26] and other some use CPW for compact antenna [27]. In this case, the Vivaldi antenna sensor is an ideal candidate for its high directive radiation patterns, compact size, and higher gain due to the antenna sensor performance from other researchers in a microwave imaging application. The Vivaldi tapered slot antenna has received considerable publicity since Gibson first offered it in 1979 [28].

A Vivaldi antenna can be designed with several techniques to enhance the performance of gain, directive radiation pattern, and directivity of the sensor with the dielectric lens in hemisphere-loaded [29], a palm tree , corrugated Vivaldi [4], irregular slot [10], metamaterial [30], and elliptical parasitic element [31]. A regular triangular slit (RTS) [8] and exponentially tapered arms [1] in antipodal Vivaldi antenna (AVA) have been used in the past. Due to its wide range of applications, the Vivaldi antenna has always been a research interest and studied to improve output parameters, such as bandwidth, radiation pattern, gain, and directivity. Recently, the Vivaldi antenna is mostly used in microwave imaging applications to enhance the performance of the antenna.

In this paper, a coplanar Vivaldi antenna sensor is proposed for a microwave imaging application. The antenna operated in the frequency bandwidth of 3-8 GHz. The antenna sensor is fabricated, and the results of the reflection coefficient, radiation pattern, gain, and directivity are compared between the measured and simulated results of the proposed antenna.

Antenna design

The antenna is mainly composed of a CPW feed with two Vivaldi patches [32]. The material is FR-4 substrate with dielectric constant ε_r=3.3. It has a copper thickness of h = 0.6 mm. The length of the embedded CPW feed is (Lo), the width of the feed line is (Fw), length aperture (La), and the gap between the ground and the feed line is (g2) to ensure impedance matching as depicted in Figure 1. The entire setup is symmetric, which means (g1) is in the center of the patch and (g2) is in the right patch's center. The gap of Vivaldi for parameters is (g1).

The length (L) and width (W) of the antenna can be calculated by using equation (1) and (2) below [33], where (c) is the speed of light, and (ε_r) is a relative permittivity. Tapered slot antennas have an exponential rate as defined in equation (3), and the mouth opening rate can be found via formula (4).

$$L \approx \frac{c}{f\sqrt{\varepsilon_r}} \quad (1)$$

$$W \approx \frac{1}{2} \times \frac{c}{f\sqrt{\varepsilon_r}} \quad (2)$$

$$y = \pm A \cdot e^{r \cdot t} \quad (3)$$

$$\pm \frac{\mathrm{MO}}{2} = \pm \frac{\mathrm{A}}{2} \times \exp^{\mathrm{r} \times \mathrm{La}} \quad (4)$$

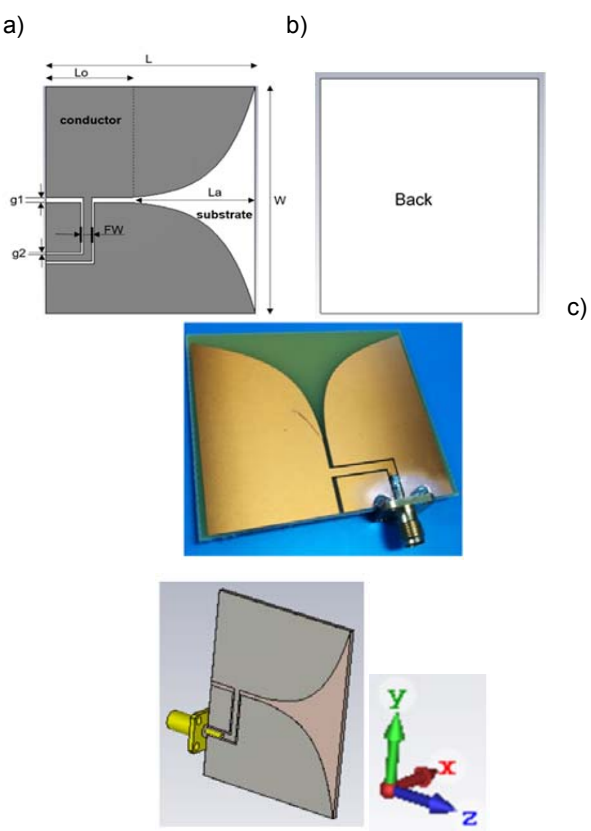

Fig.1. Design structure of the purposed antenna (a) front view and (b) back view (c) the fabricate of the purposed antenna

Table 1: Dimensions of all the parameters

Parameter	Value [mm]
L	61.03
W	50
Lo	20
g1	1.3
g2	0.54
Fw	2

The simulation study was performed using Microwave Studio Computer Simulation Technology (CST) tools. Some optimizations were accomplished during this modelling by adjusting the antenna width and length and tapered slot size parameter values. All parameters of the antenna dimensions are tabulated in Table 1.

Result

The fabricated prototype was measured using a Vector Network Analyzer (VNA). The simulated and measured return loss performance is shown in Figure 2. However, a small shift can be seen at the resonant frequency of the antenna. Reflection coefficient, S_{11} is below −10 dB over the antenna bandwidth of about 3–7.19 GHz in the simulation and 3–7.28 GHz in the measurement. The minimum reflection coefficient is -28.9 dB at 6.78 GHz in the simulation and 3.78 GHz in the measurement. The resonant frequency shifted to the right from 5.3 GHz in the measurement and to 5.7 GHz in the simulation. The difference is due to the lowest reflection coefficient changes from -20 dB in the simulation to -28.9 dB in the

measurement at 3.7 GHz and -18.9 dB in the measurement and to -28.9 dB in the simulation at 6.78 GHz.

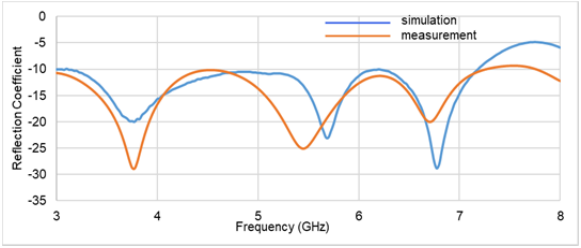

Fig.2. Reflection coefficient for the measurement and simulation result

a)

b)

c)

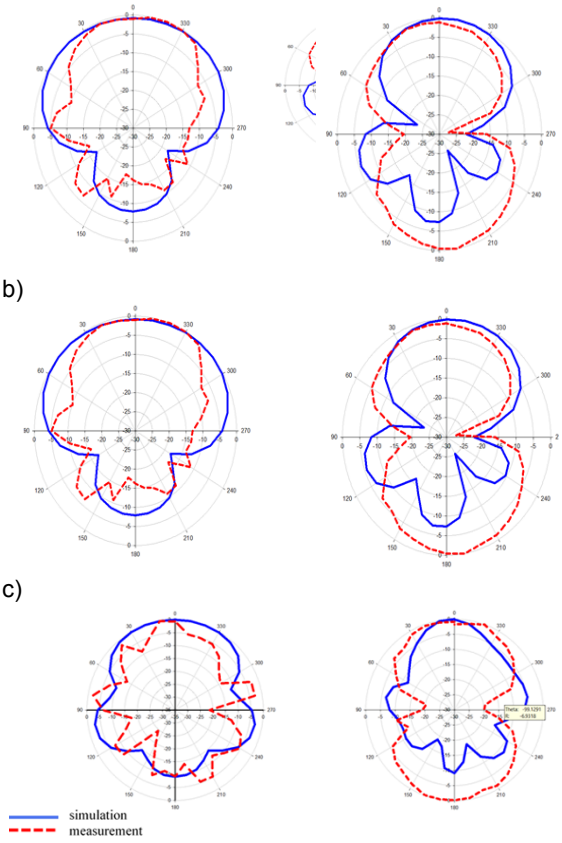

Fig.3. Simulated and measurement radiation patterns of the antenna in Phi=0° and Phi=90° planes respectively at (a) 3.7 GHz, b) 5.5 GHz and (c) 6.7 GHz

The far-field radiation characteristics of the antenna are at phi=0° and phi=90°. These antennas show the directional type of radiation pattern for 3.7 GHz, 5.5 GHz, and 6.7 GHz, as depicted in Figure 3. At the lower frequency, the large main lobe can be seen at 0°. However, when the frequency increases at 5.5 GHz, the main lobe becomes smaller. The side lobes are found in the radiation pattern when the frequency increases. It can be seen from the radiation pattern, 3 dB beamwidth decreases from 168.9° to 106.5° at phi=0°, and from 86.8° to 42° at phi=90°. The antenna performance for gain, directivity, efficiency, half-power beamwidth (HPBW), and first null beamwidth (FNBW) are tabulated in Table 2. It is evident the HPBW of the antenna at phi=0° is reduced from 168.9° to 106.5°, and at phi=90° is reduced from 86.8° to 42°. The FNBW of the antenna is reduced at phi=0° from 84.45° to 53.25°, and at phi=90° is reduced from 43.4° to 21°.

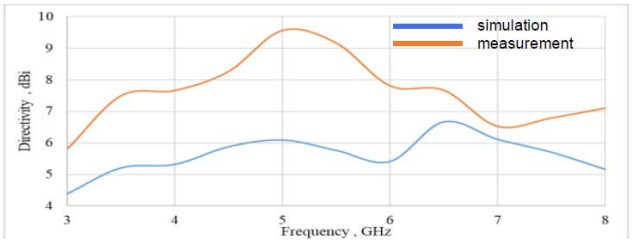

Fig.4. Simulation and measurement gain of the purposed antenna

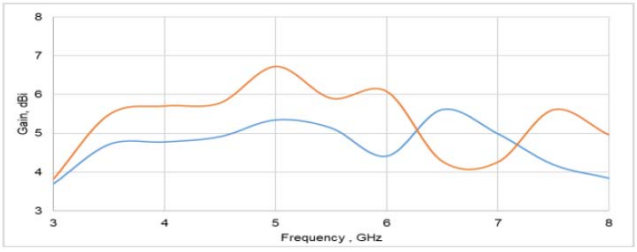

Fig.5. Simulation and measurement directivity of the purposed antenna

The maximum gain of the simulation is 5.61 dBi at 6.5 GHz and 6.72 dBi at 5 GHz for the measurement. The lowest gain is 3.7 dBi at 3 GHz in the simulation and a lower gain is 3.82 dBi at 3 GHz in the measurement. Furthermore, the gain remained over 3.5 dBi above 3-8 GHz for the simulation, as shown in Figure 4. The maximum directivity is 6.55 dBi at 6.6 GHz and the lowest directivity is 4.4 dBi at 3 GHz in the simulation, as depicted in Figure 5. The measurement results exhibit the maximum directivity of 9.59 dBi at 5.1 GHz, and the lowest directivity is 5.8 dBi at 3 GHz. The antenna's efficiency is less than 90% at 5.5 GHz and 6.7 GHz, as tabulated in Table 3. However, the antenna efficiency exceeds 90% at a lower frequency of 3.7 GHz (91.93%).

Table 3: Gain, directivity and the efficiency of the antenna

Frequency, GHz	Gain (dBi)		Directivity(dBi)		Efficiency, %
	Sim	Mea	Sim	Mea	
323.7	4.89	5.54	5.33	7.48	91.93
5.5	5.14	5.9	5.77	9.17	89.25
6.7	5.6	4.9	6.54	6.92	86.39

Sim= simulation, *Mea*= measurement

Conclusion

In this paper, a compact CPW of the Vivaldi antenna is presented. The overall dimension of the proposed antenna is 61.03 mm×50 mm. The antenna prototype is achieved with a −10 dB wider bandwidth from the frequency range of 3–7.28 GHz (83.33%) in the operating band. The measured results evidently showed that the antenna could reach a maximum gain of approximately 6.72 dBi and maximum directivity at 9.59 dBi. In a nutshell, the proposed antenna sensor can be used for microwave imaging applications.

ACKNOWLEDGEMENT

This research study is sponsor by the Malaysian Ministry of Education under the Hadiah Latihan Persekutuan (HLP) scheme. The authors would like to thank Universiti Teknikal Malaysia Melaka (UTeM) for supporting this research work under the grant PJP/2019/FKEKK-CETRI/CRG/S01650. We also would like to thank the Faculty of Electronics and Computer Engineering and Faculty of Electrical and Electronic Engineering Technology at UTeM for supporting this research.

***Authors**: Nuruliswa Abdullah, Faculty of Electronic and Computer Engineering, Universiti Teknikal Malaysia Melaka, Hang Tuah Jaya, 76100 Durian Tunggal, Melaka, Malaysia, E-mail: m02191003@student.utem.edu.my. Associate Profesor Dr.*

Mohamad Zoinol Abidin Abd Aziz, Faculty of Electronic and Computer Engineering, Universiti Teknikal Malaysia Melaka, Hang Tuah Jaya, 76100 Durian Tunggal, Melaka, Malaysia, E-mail: mohamadzoinol@utem.edu.my. Dr. Abd Shukur Jaafar, Faculty of Electronic and Computer Engineering, Universiti Teknikal Malaysia Melaka, Hang Tuah Jaya, 76100 Durian Tunggal, Melaka, Malaysia, E-mail: abdshukur@utem.edu.my.

REFERRENCE

[1] Abbak, M. et al. (2017) 'Wideband compact dipole antenna for microwave imaging applications', IET Microwaves, Antennas and Propagation, 11(2), pp. 265–270. doi: 10.1049/iet-map.2016.0151.

[2] Akhter, Z., Abhijith, B. N. and Akhtar, M. J. (2016) 'Hemisphere lens-loaded Vivaldi antenna for time domain microwave imaging of concealed objects', Journal of Electromagnetic Waves and Applications. Taylor & Francis, 30(9), pp. 1183–1197. doi: 10.1080/09205071.2016.1186574.

[3] Alsariera, H. et al. (2020) 'Compact CPW-fed broadband circularly polarized monopole antenna with inverted L-shaped strip and asymmetric ground plane', Przeglad Elektrotechniczny, 96(4), pp. 53–56. doi: 10.15199/48.2020.04.10.

[4] Amdaouch, I., Aghzout, O. and Alejos, A. V. (2019) 'Confocal microwave imaging algorithm for breast cancer detection based on a high directive corrugated vivaldi antenna pulses', 2019 International Conference on Wireless Technologies, Embedded and Intelligent Systems, WITS 2019. IEEE, pp. 1–5. doi: 10.1109/WITS.2019.8723680.

[5] Amjadi, H. and Hamedani, F. T. (2011) 'Ultra wideband horn antenna for microwave imaging application', Proceedings of 2011 Cross Strait Quad-Regional Radio Science and Wireless Technology Conference, CSQRWC 2011, 1, pp. 337–340. doi: 10.1109/CSQRWC.2011.6036953.

[6] Conceição, R. C. et al. (2020) 'Classification of breast tumor models with a prototype microwave imaging system', Medical Physics, 47(4), pp. 1860–1870. doi: 10.1002/mp.14064.

[7] Elevani, D. et al. (2017) 'On the performance of algebraic reconstruction technique algorithm for microwave imaging', APCAP 2016 - 2016 IEEE 5th Asia-Pacific Conference on Antennas and Propagation, Conference Proceedings, 4, pp. 85–86. doi: 10.1109/APCAP.2016.7843111.

[8] Gibson, P. . (1979) 'The Vivaldi Aerial', 1979 9th European Microwave Conference, Brigthon,UK, pp. 101–105.

[9] Hazarika, P., Santorelli, A. and Popovic, M. (2016) 'Investigation of antenna array configurations for microwave radar breast screening', 2016 17th International Symposium on Antenna Technology and Applied Electromagnetics, ANTEM 2016. doi: 10.1109/ANTEM.2016.7550230.

[10] Islam, M. T. et al. (2017) 'Microwave Breast Phantom Measurement System with Compact Side Slotted Directional Antenna', IEEE Access, 5(c), pp. 5321–5330. doi: 10.1109/ACCESS.2017.2690671.

[11] Islam, M. T. et al. (2018) 'A compact slotted patch antenna for breast tumor detection', Microwave and Optical Technology Letters, 60(7), pp. 1600–1608. doi: 10.1002/mop.31215.

[12] Islam, Md Tarikul et al. (2019) 'Metamaterial Inspired High Gain Antenna for Microwave Breast Imaging', APACE 2019 - 2019 IEEE Asia-Pacific Conference on Applied Electromagnetics, Proceedings. IEEE, (November), pp. 1–4. doi: 10.1109/APACE47377.2019.9020819.

[13] Islam, T. et al. (2018) 'Computational analysis of Microwave Imaging (MWI) System for Post Stroke Screening Using Unidirectional Antenna', 2018 International Conference on Innovations in Science, Engineering and Technology (ICISET), Chittagong, Bangladesh, pp. 447–450.

[14] Karim, M. N. A. et al. (2016) 'Wideband slotted antenna for microwave imaging system in ground penetrating radar applications', ISSE 2016 - 2016 International Symposium on Systems Engineering - Proceedings Papers. doi: 10.1109/SysEng.2016.7753172.

[15] Khoomwong, E. and Phongcharoenpanich, C. (2020) 'A Dual-Wideband Crossed Elliptical Disc Antenna with Reconfigurable Radiation Patterns for Multiband Applications', (4), pp. 43–48. doi: 10.15199/48.2020.04.08.

[16] Lamultree, S. et al. (2021) 'An Ultra-Wideband Rectangular Monopole with Circular Ring Antenna for Wireless Communication Applications', Przegląd Elektrotechniczny, pp. 10–13. doi: 10.15199/48.2021.01.02.

[17] Laviada, J. et al. (2018) 'Real-Time Multiview SAR Imaging Using a Portable Microwave Camera with Arbitrary Movement', IEEE Transactions on Antennas and Propagation, 66(12), pp. 7305–7314. doi: 10.1109/TAP.2018.2870485.

[18] Lin, X. et al. (2020) 'Ultra-Wideband Textile Antenna for Wearable Microwave Medical Imaging Applications', IEEE Transactions on Antennas and Propagation, (c), pp. 1–1. doi: 10.1109/tap.2020.2970072.

[19] Liu, C. et al. (2019) 'A Compact, Uniplanar Vivaldi Antenna with an Embedded CPW Feed', 2019 Cross Strait Quad-Regional Radio Science and Wireless Technology Conference (CSQRWC). IEEE, pp. 1–3. doi: 10.1109/csqrwc.2019.8799265.

[20] Mahdi Moosazadeh, S. K. and Joseph T. Case, and B. S. (2017) 'UWB Antipodal Vivaldi Antenna for Microwave Imaging of Construction Materials and Sturctures', Microwave and Optical Technology Letters, 59(6), pp. 1259–1264. doi: 10.1002/mop.

[21] Maruddani, B., Sandi, E. and Salam, M. F. N. (2018) 'Design and Implementation of Low-cost Wideband Vivaldi Antenna for Ground Penetrating Radar', KnE Social Sciences, pp. 498–506. doi: 10.18502/kss.v3i12.4118.

[22] Mobashsher, A. T. and Abbosh, A. M. (2016) 'Compact 3-D Slot-Loaded Folded Dipole Antenna with Unidirectional Radiation and Low Impulse Distortion for Head Imaging Applications', IEEE Transactions on Antennas and Propagation, 64(7), pp. 3245–3250. doi: 10.1109/TAP.2016.2560909.

[23] Mobashsher, Ahmed Toaha and Abbosh, A. M. (2016) 'Performance of directional and omnidirectional antennas in wideband head imaging', IEEE Antennas and Wireless Propagation Letters, 15(c), pp. 1618–1621. doi: 10.1109/LAWP.2016.2519527.

[24] Mukherjee, S. et al. (2019) 'A Time Reversal-Based Microwave Imaging System for Detection of Breast Tumors', IEEE Transactions on Microwave Theory and Techniques. IEEE, PP, pp. 1–14. doi: 10.1109/TMTT.2019.2902555.

[25] Porter, E. et al. (2016) 'A Wearable Microwave Antenna Array for Time-Domain Breast Tumor Screening', IEEE Transactions on Medical Imaging, 35(6), pp. 1501–1509. doi: 10.1109/TMI.2016.2518489.

[26] Rahiman, M. H. F. et al. (2019) 'Microwave tomography sensing for potential agarwood trees imaging', Computers and Electronics in Agriculture. Elsevier, 164(April), p. 104901. doi: 10.1016/j.compag.2019.104901.

[27] Rokunuzzaman, M., Samsuzzaman, M. and Islam, M. T. (2017) 'Unidirectional Wideband 3-D Antenna for Human Head-Imaging Application', IEEE Antennas and Wireless Propagation Letters, 16(c), pp. 169–172. doi: 10.1109/LAWP.2016.2565610.

[28] Salleh, A. et al. (2019) Development of antipodal Vivaldi antenna for microwave brain stroke imaging system, International Journal of Engineering &Technology. Available at: www.sciencepubco.com/index.php/IJET.

[29] Samsuzzaman, M. et al. (2019) 'A 16-modified antipodal Vivaldi antenna array for microwave-based breast tumor imaging applications', Microwave and Optical Technology Letters, pp. 2110–2118. doi: 10.1002/mop.31873.

[30] Shao, W. et al. (2018) 'A Time-Domain Measurement System for UWB Microwave Imaging', IEEE Transactions on Microwave Theory and Techniques, 66(5), pp. 2265–2275. doi: 10.1109/TMTT.2018.2801862.

[31] Tobon Vasquez, J. A. et al. (2019) 'Design and experimental assessment of a 2D microwave imaging system for brain stroke monitoring', International Journal of Antennas and Propagation, 2019. doi: 10.1155/2019/8065036.

[32] Usman, M. et al. (2019) 'Design of compact ultra-wideband monopole semi-circular patch antenna for 5G wireless communication networks', Przeglad Elektrotechniczny, 95(4), pp. 223–226. doi: 10.15199/48.2019.04.42.

[33] Wang, F. and Arslan, T. (2017) 'A thin-film-based wearable antenna array for breast microwave imaging and diagnosis', 2017 1st IEEE MTT-S International Microwave Bio Conference, IMBioC 2017. doi: 10.1109/IMBIOC.2017.7965776.